

Effect of pressure on optical properties of crystalline As_2S_3

J. M. Besson

*Laboratoire de Physique des Solides, * Université Pierre-et-Marie-Curie, 4 Place Jussieu, 75230 Paris, France
and Département des Hautes Pressions, Université Pierre-et-Marie-Curie, 4 Place Jussieu, 75230 Paris, France*

J. Cernogora

*Groupe de Physique des Solides de l'École Normale Supérieure, * Université Paris VII, 2 Place Jussieu, 75221 Paris, France*

R. Zallen

Xerox Webster Research Center, Webster, New York 14580

(Received 4 February 1980)

Crystalline As_2S_3 (orpiment) is a layer-structure semiconductor whose optical properties, under ordinary conditions, are determined by its diperiodic layer symmetry. We have investigated the effect of hydrostatic pressure on the optical-absorption edge and the Raman scattering spectrum of orpiment. With increasing pressure the optical band gap red-shifts rapidly, decreasing from 2.7 eV at $P = 0$ to 1.6 eV at 100 kbar. The initial slope, dE_G/dP at $P = 0$, is $-(14 \pm 3)$ meV/kbar, and the closing of the gap is interpreted in terms of pressure-induced enhancement of the interlayer-interaction broadening of intralayer bands. At high pressure, dimensionality effects (2D \rightarrow 3D) are clearly discerned in the vibrational Raman spectrum. An intralayer quadruplet at 355 cm^{-1} , near degenerate at zero pressure, disperses at high pressure as the dominance of the diperiodic (isolated layer) symmetry is broken and the admixture repulsion of modes of like *crystal* symmetry forces them apart. A similar effect occurs at 25 kbar in the forbidden-cross-over repulsion of a pair of modes at 145 cm^{-1} . Also, the rigid-layer modes roughly double in frequency by 100 kbar, corresponding to a quadrupling of the layer-layer coupling. Finally, the pressure data have been used to separate the phonon-occupation-driven (explicit) and the volume-driven (implicit) contribution to the *temperature* dependence of the band gap and the Raman-active phonon frequencies. We find that E_G is controlled by the explicit electron-phonon contribution to dE_G/dT . For the phonons, dv/dT of the low-frequency interlayer-interaction modes is dominated by the volume-driven term, while the explicit phonon-phonon effect dominates dv/dT for the intralayer modes.

I. INTRODUCTION

Crystalline As_2S_3 (orpiment) is a layer-structure crystal^{1,2} whose optical properties have, in recent years, been intensively investigated, both in the electronic (visible, ultraviolet, x-ray) and vibrational (infrared, Raman) spectral regimes. Among the various reasons for the high level of interest in this semiconducting layer crystal, two stand out as being of special importance.

(1) Orpiment is notable as the layer crystal for which the crucial role of the *diperiodic*²⁻⁴ symmetry (the proper factor-group symmetry of an individual two-dimensionally-extended "macro-molecule") was first appreciated and analyzed.² The dominance of the layer symmetry (and, conversely, the minor *subsidiary* role played by the conventional, triperiodic, crystal symmetry) in determining the optical properties of As_2S_3 was established, for its vibrational spectra, in 1971. In brief, the observation of many degenerate or near-degenerate Raman-infrared lines, incomprehensible from the viewpoint of the crystal symmetry, was well explained on the basis of the diperiodic layer symmetry.²

(2) Orpiment, as well as the isomorphic crystal As_2Se_3 , has served as a valuable crystalline

analog of the important chalcogenide glasses of the same chemical composition and short-range order. Amorphous As_2S_3 and As_2Se_3 are bulk glasses of considerable technological significance as infrared-transmitting window materials and as visible-sensitive large-area photoconductors. From a fundamental viewpoint, intense activity on the spectroscopy of these glasses has been central to recent developments in the physics of amorphous solids. The relationship between the nearest-neighbor bonding topologies of crystalline and amorphous As_2S_3 is essentially that envisaged by Zachariasen in his classic 1932 paper that describes what has since become known as the "continuous-random-network model" for the structure of glasses.⁵ Spectral comparisons between the crystalline and amorphous forms of As_2S_3 have proved to be highly useful for gaining insight about elementary excitations in both solids,⁶⁻⁹ with the crystalline partner generally serving as a firm base from which to launch attacks on the less-well-understood amorphous phase.

Experiments which has thus far been reported for As_2S_3 crystals include, for the vibrational optical properties, infrared reflectivity and absorption in both the fundamental^{2,10} and two-phonon⁹ regimes, Raman scattering^{2,11} and its tem-

perature dependence,^{12,13} neutron scattering,¹⁴ and pressure-Raman experiments to 9 kbar.¹⁵ For the electronic optical properties, work has been reported on the absorption and reflectivity in the visible and ultraviolet,^{6,16} photoconductivity in the absorption-edge region,^{17,18} and (in the energy equivalent of the far ultraviolet) x-ray photoemission¹⁹ and electron energy loss.²⁰ In addition, transport studies have been reported which describe time-of-flight mobility measurements perpendicular to the layer planes.^{18,21}

In the present paper, we report results of optical experiments carried out on crystalline As_2S_3 at high hydrostatic pressure (to ~ 100 kbar). Both the electron and the phonon regimes have been studied: Measurements have been made of the effect of pressure on the optical absorption edge, and on the Raman scattering spectrum.

A major motivation for this work was to probe dimensionality effects by altering, via pressure, the relative importance of the two-dimensional and three-dimensional aspects of this prototype layer crystal. While the diperiodicity dominates at $P=0$, allowing a weak-coupling picture (nearly noninteracting layers) to adequately describe the low-pressure spectra,² at high pressure the layers are forced to interact more strongly so that the layer symmetry should begin to be appreciably broken by the subsidiary but increasing importance of the crystal symmetry. In this paper we report clear evidence that, at pressures of the order of 100 kbar, the weak-coupling regime is definitely left behind and the crystal symmetry exerts a major influence. Such pressure-induced effects of *substantial* interlayer coupling are reported here, for the first time, for the phonon spectrum of the solid. For the electronic spectrum, the increased coupling accounts for the sign and size of the extremely large pressure-induced bandgap shift.

Another motivation was to see if a solid-state phase transition takes place in the investigated range of pressure. It does not. As_2S_3 is unusual in that, unlike the majority of layer crystals, it does not exhibit any polytypism (polymorphism involving rearrangements of the layer stacking) at ambient conditions. This can be attributed to the structural complexity (low symmetry, large unit cell) of the individual layer in orpiment. The layer stacking in the orpiment structure can be roughly visualized as the "thick" portions of one layer nesting over the "thin" portions of the next. Evidently this fitting-together can be efficiently achieved in only one way; there is no energetically competitive layer-sequence multiplicity as there is for high-symmetry systems such as PbI_2 , TaS_2 , and GaSe . The absence of a solid-state phase

transition to 100 kbar confirms the remarkable stability of the layer stacking in As_2S_3 . At higher pressure, any transition (such as the inevitable one to the metallic state) would almost certainly involve bond reconstruction of the layer itself.

We have observed pronounced effects of pressure on the electronic and vibrational properties of orpiment. Although it remains semiconducting to >100 kbar, the optical bandgap is observed to red-shift dramatically, shifting from the blue to the near-infrared. Significant changes are also seen in the zone-center optical phonon spectrum. Following a description of the experimental techniques in Sec. II, the results and their interpretation are presented in Sec. III for the electronic regime and in Sec. IV for the vibrational regime. In Sec. V the pressure results are used to dissect the corresponding temperature dependences into their explicit (phonon-occupation-driven) and implicit (thermal-expansion-driven) components. A brief summary of the main points is given in Sec. VI.

II. EXPERIMENTAL

The samples used in this work were taken from microcrystals of natural orpiment (from Zareh Schuran, Iran) which had been separated from the ore by etching with hydrofluoric acid. They were provided by A. Rimsky (Mineralogy and Crystallography Laboratory, Pierre and Marie Curie University), who also carried out x-ray measurements to check that their lattice parameters matched those for crystalline As_2S_3 . The small crystal slabs that were placed in the diamond anvil cell had been carefully cleaved with a razor blade perpendicular to the b axis (parallel to the a - c layer plane, along which orpiment cleaves very easily). Except for the observation of the optical anisotropy for light polarized in the a - c plane (and, of course, the absorption-edge and Raman-scattering measurements reported here, which agree with the known spectra of As_2S_3 at STP), no other characterizations were made.

Optical measurements as a function of hydrostatic pressure were performed by means of the gasketed, ruby-calibrated, diamond-anvil-cell technique,²² using a cell built by us²³ after designs by G. Piermarini and S. Block of the National Bureau of Standards (Washington). The pressure fluid was the standard ethanol-methanol mixture.²²

Sample dimensions in the plane of the cell (normal to the optical path) were limited by the gasket hole, and were typically about 200 micrometers. The thickness was 8 micrometers for optical absorption and 15–25 micrometers for Raman scattering. The latter dimensions were found to be

adequate for Raman experiments (carried out in a back-scattering geometry) using the 6471-Å line of a krypton laser, since As_2S_3 is a strong Raman scatterer. This laser line was chosen because it lies within the transparent regime of the crystal, is low enough in photon energy to induce only a negligible amount of luminescence in the diamond anvils, and yet is high enough in photon energy to excite the ruby luminescence needed for determination of the pressure. Power incident on the cell was kept below 80 mW, and no evidence of sample damage was seen. All of the effects observed were reversible with pressure. Transmission measurements were done under a Leitz microscope using unpolarized light. A crystal region about 50 micrometers in diameter was selected for optical transmission by means of an iris placed at the image position in the focal plane of the objective. Scattered light limited the minimum observable transmittance to about 10^{-3} . In both sets of experiments a Coderg T800 triple monochromator was used. Compressibility measurements along the a and c crystal axes were made by direct scaling of photographs taken at different pressures, under the same optical conditions.

III. EFFECT OF PRESSURE ON THE ABSORPTION EDGE

Figure 1 shows the pressure dependence of the optical transmission of an As_2S_3 crystal about 8 micrometers thick (at $P=0$). Incident light is normal to the layer plane, propagating parallel to the crystal b axis. Because of the difficulty of working with a very small sample in the diamond cell, the observed transmission curve corresponds to a mixture of the $E||a$ and $E||c$ polarizations.

This is the reason for presenting the measured transmission rather than a calculated absorption coefficient; a calculation of α is not justified here.

At room temperature and zero pressure, it is known that the absorption curve for $E||a$ is shifted upward in energy (by about 0.1 eV at $\alpha = 5 \times 10^3 \text{ cm}^{-1}$) relative to that for $E||c$.⁶ If this situation is assumed to hold also at high pressure, then at the lowest transmission values (highest plotted points in the format of Fig. 1) the curves should approach characteristics corresponding to $E||a$ as the other more-highly-absorbed polarization cuts out. The upper part of Fig. 1 corresponds to absorption coefficients of the order of $(5-10) \times 10^3 \text{ cm}^{-1}$.

Although the absolute value of $E_G(P)$ is not accurately known from our measurements, the variation with pressure is well represented by the variation of the absorption edge, especially at low pressures where this edge simply shifts in energy without appreciably changing its shape. This shift $\Delta h\nu(P)$ is shown, in the inset in Fig. 1, for a transmission of 0.02. The initial slope of this isotransmission plot can be used to yield an estimate of the pressure sensitivity (in eV/bar) of the bandgap at $P=0$ and $T=300 \text{ K}$,

$$\frac{\partial E_G}{\partial P} = -(14 \pm 3) \times 10^{-6}.$$

To interpret this result for the bandgap pressure coefficient, we should first note that pressure coefficients are generally positive for three-dimensional-network semiconductors of the germanium family,²⁴ while a negative value of $\partial E_G/\partial P$ has been found, not only for As_2S_3 , but also for other layer-structure semiconductors in the relatively few cases in which pressure experiments on

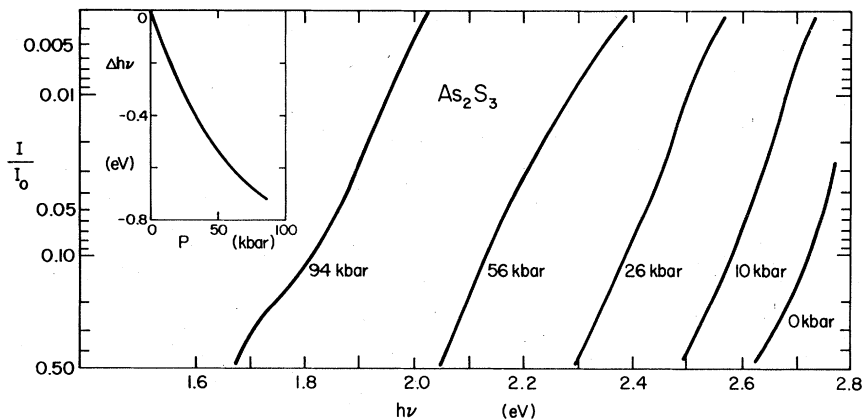


FIG. 1. Absorption edge of an orpiment sample at several pressures (at 300 K). The transmission of an As_2S_3 crystal 8 micrometers thick is shown plotted (on a logarithmic scale, with values increasing from top to bottom) against photon energy for unpolarized light propagating parallel to the b axis. The inset shows the pressure dependence of the shift in energy of the edge, for photon energy corresponding to a transmission of 0.02.

such solids have been reported.²⁵⁻²⁷

We propose an argument for the frequent occurrence of $\partial E_G/\partial P < 0$ in layer crystals by means of the schematic energy-level diagrams sketched in Fig. 2.^{18,25} Let us suppose that a single isolated layer possesses a (two-dimensional) band structure in which $E_0^c(r_0)$, $E_0^v(r_0)$, and $E_G(r_0) = E_0^c(r_0) - E_0^v(r_0)$ are the energies of the conduction-band minimum, the valence-band maximum, and the bandgap, respectively. Here r_0 is the covalent bond length (in orpiment, the As-S nearest-neighbor distance), the key parameter characterizing the layer's internal structure. Now we turn on the interlayer interaction (in the familiar condensation-type *gedanken* experiment) by bringing together a large assembly of layers from an initially infinite layer-layer separation to a final separation r_1 corresponding to the actual layer stacking in the crystal. The new bandgap is denoted in Fig. 2(b) by $E_G(r_0, r_1)$; the bandgap of the isolated layer is denoted in Fig. 2(a) by $E_G(r_0, r_1 = \infty)$. (Both here and in the following phonon section, we indicate an *interlayer* quantity by the subscript 0 and an *interlayer* quantity by the subscript 1.¹⁵)

In the "condensation" of macromolecules from the isolated-layer "gas" of Fig. 2(a) to the solid state of Fig. 2(b), each electronic level of the individual layer spreads out into a band of levels as the Brillouin zone develops a third dimension normal to the original two-dimensional zone. The bandwidths for the bands which evolve from the two single-layer states that bounded the original bandgap have been labeled $E_1^c(r_1)$ and $E_1^v(r_1)$ in Fig. 2(b). These bandwidths depend on r_1 , vanishing for $r_1 = \infty$ and increasing with decreasing r_1 .

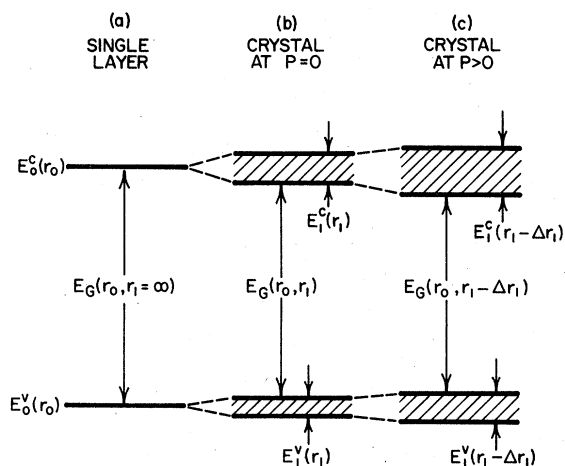


FIG. 2. Enhancement of interlayer interaction (shaded splittings) by pressure, indicated on a schematic energy-level diagram (after Ref. 18).

Figure 2(c) suggests what happens when hydrostatic pressure is applied. Pressure appreciably shortens the very soft interlayer bonds ($r_1 - r_1 - \Delta r_1$), but has negligible effect on the stiff bond length r_0 . Lattice-vibrational studies of layer crystals reveal that $\Delta r_0/r_0$ is an order of magnitude (or more) smaller than $\Delta r_1/r_1$. Thus the bandgap under pressure may be regarded, to lowest order, as $E_G(r_0, r_1 - \Delta r_1)$. It is reduced from the value of the zero-pressure gap $E_G(r_0, r_1)$ because of the increased interlayer-overlap bandwidths $E_1^c(r_1 - \Delta r_1)$ and $E_1^v(r_1 - \Delta r_1)$, hence the negative dE_G/dP .

When two (or more) layers intersect the crystal unit cell, another interlayer-interaction band-structure effect is superimposed on the one described above. This was first noted by Lisitsa *et al.*²⁸ who proposed it as the electronic analog of the vibrational Davydov splitting observed for As_2S_3 and As_2Se_3 by Zallen, Slade, and Ward.² To visualize it, we may again use Fig. 2(b) but with each pair of levels representing, not the extrema of a band of energies for states dispersed along an axis in k space (as in the previous discussion), but to a discrete pair of energies at the *same* k vector. Such doublets should give rise to multiplets or fine structure in the direct-transition interband spectra. Again, the increased splittings induced by hydrostatic pressure act to decrease E_G .

The situations described in the preceding two paragraphs are not distinct in an essential way but are simply two closely-related aspects of the band structure that reflect the *lifting of degeneracies by interlayer interaction*. Pressure enforces enhanced interaction and *increases the interlayer splittings*. Since orpiment has two layers per crystal unit cell^{1,2} and is a direct-gap material exhibiting (at low temperature) multiplet structure near the electronic threshold,⁵ the second description given above is probably the appropriate one. Just this mechanism has been shown to apply to GaSe,²⁵ the direct gap in that case being at the zone center (Γ point). These arguments thus imply that $\partial E_G/\partial P$ is expected to be negative for 2D-network semiconductors and, in fact, for 1D-network and 0D-network semiconductors as well.²⁹ (Replace "interlayer" in the previous discussion by "interchain" or "intermolecular," respectively).

No band-structure calculations have been reported for As_2S_3 , but two have recently appeared for its isomorphous cousin As_2Se_3 .^{30,31} Since the optical spectra in the fundamental absorption regime imply an approximate rigid-band relationship between the electronic structures of the two crystals,⁶ the As_2Se_3 calculations should have relevance to As_2S_3 . The detailed work of Althaus *et al.*³¹ indicates that the direct gap is at Γ . Their paper is

also of interest with respect to the bonding ancestry of the bands. The conventional-wisdom view of chalcogenide crystals and glasses is that the valence band is formed from lone-pair nonbonding orbitals and the conduction band from antibonding orbitals.^{32,33} Althaus *et al.* find that in crystalline As_2Se_3 the nonbonding character of the valence band is lost by extensive mixing with bonding orbitals. This explains the large number of electrons which contribute to the first main ultraviolet absorption band in As_2Se_3 , and since the corresponding band in As_2S_3 exhibits the same oscillator-strength property⁶ (larger than expected, unless hybridization is invoked), the same conclusion should also apply to As_2S_3 . Note that a nonbonding valence band in a layer-structure chalcogenide semiconductor should be quite pressure-sensitive, since the lone-pair orbitals largely protrude into the compressible interlayer space. Although the broadening of the conduction band in Fig. 2 is indicated as greater than that of the valence band, that was an arbitrary choice and the reverse may be true.³⁴

The result reported here for crystalline As_2S_3 , namely the room-temperature pressure coefficient of $-(14 \pm 3) \times 10^{-6}$ eV/bar, can be compared to the value of this quantity for amorphous As_2S_3 .³⁵ For $\alpha\text{-As}_2\text{S}_3$, the optical bandgap shifts at a rate of $-(18 \pm 2) \times 10^{-6}$ eV/bar. Thus the effect of pressure on the gap is essentially the same for the crystalline and amorphous forms of As_2S_3 . This situation was found earlier for c - and $\alpha\text{-As}_2\text{Se}_3$.²⁷ It is strong evidence that these chalcogenide glasses are macromolecular in nature,⁸ subject to arguments similar to those given above for explaining the large pressure-induced red shift of the crystalline edges. Of course, the band-structure k space context is absent for the glasses, the pressure-enhanced overlap broadening being applied to spectral bands which are characteristic of the weakly interacting individual units. The presence or absence of long-range order is not important here; the key aspect, common to both crystal and glass, is the presence in the solid of discrete molecules or macromolecules.

IV. EFFECT OF PRESSURE ON THE RAMAN SPECTRUM

The earlier pressure-Raman study of orpiment by Zallen,¹⁵ carried out with a conventional Bridgman-type hydraulically driven optical bomb, was limited to 9 kbar. It was primarily concerned with the initial slopes $d\nu/dP$ of the pressure dependences of the phonon frequencies ν , and the results were helpful in establishing a vibrational scaling

law for molecular crystals that has since been supported by work on other systems.³⁶ In the present experiments with the anvil cell, the pressure range has been extended by an order of magnitude to well beyond the "linear-response" regime of pressure effects. The upper limit of about 100 kbar was set by the eventual loss of Raman-scattering signal, as the sample became too absorbing because of the shift (described in the preceding section) of the edge into the infrared.

Figure 3 displays the observed $\nu(P)$ trajectories for Raman-active phonons in As_2S_3 . (A few of the weaker lines seen in other studies^{2,11-13,15} could not be monitored here because of the small sample size in the anvil cell.) A detail of the evolution under pressure of an interesting portion of the Raman spectrum is shown in Figs. 4 and 5.

The two lowest-frequency lines in As_2S_3 , at 25 and 36 cm^{-1} , have been identified as rigid-

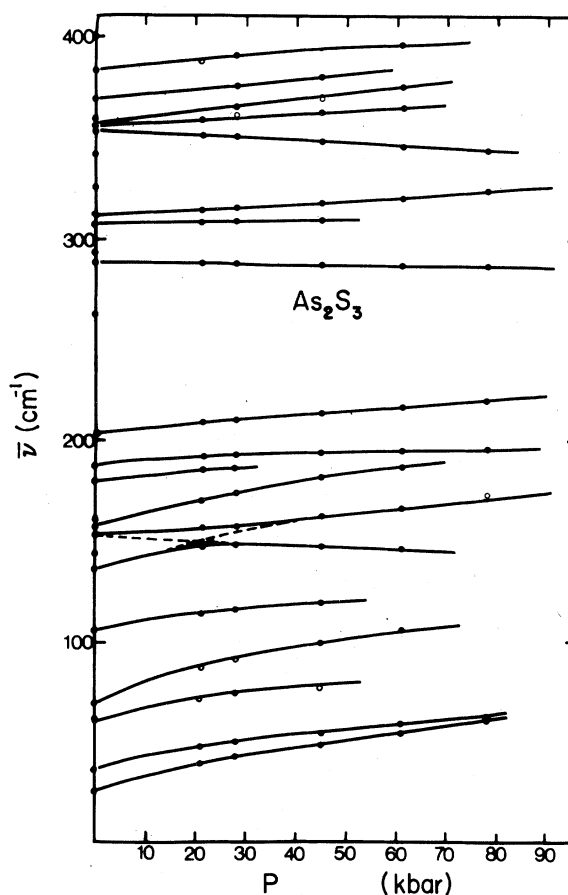


FIG. 3. Pressure dependence of Raman-active phonon frequencies in As_2S_3 (300 K). The open circles denote results of our experiments; filled circles at $P=0$ are from Ref. 11 (Razetti and Lottici); and the lines between 0 and 8 kbar correspond to Ref. 15. Dashed lines denote the (forbidden) "crossing" of the 136 and 154 cm^{-1} modes.

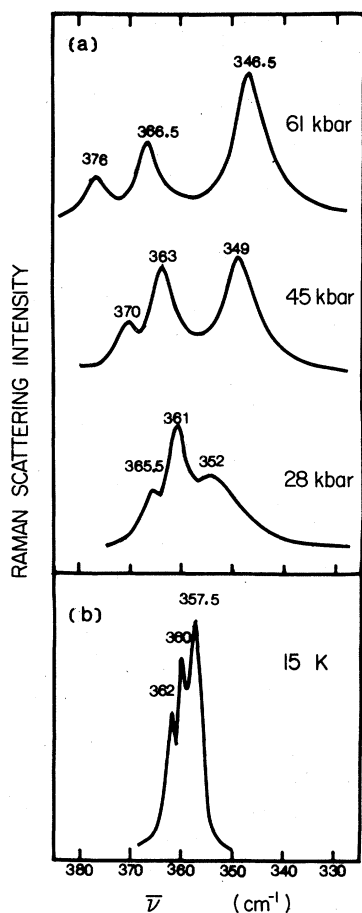


FIG. 4. Raman spectra produced by the multiplet of intralayer modes near 355 cm^{-1} : (a) spreading apart rapidly under hydrostatic pressure (at 300 K); (b) at low temperature and $P=0$ (Ref. 13). As discussed in the text, the high-frequency components of the high-pressure and the $P=0$ "triplets" are *not* the same: The 362-cm^{-1} line in (b) weakens and disappears at *high* pressure, while the high-frequency line in (a) (at 376 cm^{-1} at 61 kbar) is unobservably weak at *low* pressure. Because the multiplet is so tightly spaced at zero pressure, a spectrum observed at 15 K (at which temperature the lines become considerably sharper) was used in (b) in order to clearly reveal the structure at $P=0$.

layer (RL) modes whose restoring forces are supplied primarily by the weak interlayer forces.¹³ As expected, these modes experience the greatest fractional increase under pressure. At 80 kbar they have both increased to about 60 cm^{-1} , roughly a doubling in frequency corresponding to a quadrupling in force constant.³⁷ The fact that they approach each other in frequency reflects the overall decrease in bonding anisotropy produced by hydrostatic pressure. Of course the main aspect of the decreased anisotropy under compression is the reduction in the disparity between the stiffness of

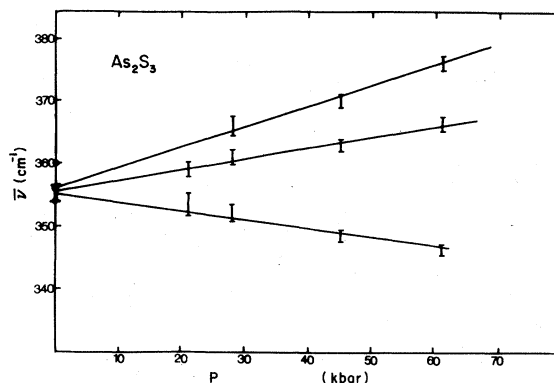


FIG. 5. Detail of the pressure dependences near 355 cm^{-1} . Filled circles are reported zero-pressure values (see Fig. 3). The high-frequency line seen at high pressure does *not* extrapolate to the 360-cm^{-1} zero-pressure line, and its intensity (estimated, as a fraction of the integrated intensity of the triplet, by deconvolution of the spectra of Fig. 5) decreases with decreasing pressure from 12% at 61 kbar to 6% at 28 kbar to less than 2% at $P=0$.

the intralayer and interlayer bonds, as the latter gain on the former at high pressure, causing the crystal to become more "three dimensional" in a bonding sense.

The high-frequency region near 360 cm^{-1} , shown in Figs. 4 and 5, contains intralayer bond-stretching modes. A triplet of lines is seen which split apart under pressure. These figures illustrate a complementary aspect of low temperature (at $P=0$) and high pressure (at $T=300 \text{ K}$): Low temperature permits the resolution of structure via line narrowing at constant splitting, while high pressure reveals structure via increased splitting at constant linewidth.³⁶

At $P=0$, this triplet can be well observed at 15 K.¹³ At room temperature and pressure, we could not resolve it under the conditions of our experiments, but we can make use of the values reported by Razetti and Lottici¹¹: 354 , 356 , and 360 cm^{-1} . Extrapolation of the observed high-pressure frequencies to zero pressure (Fig. 5) shows that they correspond to the lower *two* components at 354 and 356 cm^{-1} but, within our experimental error, *not* to the upper 360-cm^{-1} component. We therefore infer the presence of a *quadruplet*, one component of which becomes stronger at higher pressure. This component corresponds to the highest $\nu(P)$ line in Fig. 5, which has a slope of $0.3 \text{ cm}^{-1} \text{ kbar}^{-1}$. The observed intensity of this mode, relative to the total Raman intensity of the "triplet," increases smoothly with pressure. Conversely, extrapolating back its intensity shows that it contributes less than 2% of the Raman efficiency of the "triplet" at zero pres-

sure. It is thus not observable at $P=0$, even at low temperature. In contrast to this, the fate (at high pressure) of the mode which, at $P=0$, is seen at 360 cm^{-1} is uncertain because above 30 kbar (where it might have sufficiently split away from its partners to be unambiguously identified) it is no longer observable. Its intensity has certainly decreased, in the same way as several other modes that we observed in this study, and its disappearance may also have been accelerated by a weakly positive, or even negative, pressure coefficient which would cause it to drown under the Raman peaks of its stronger companions. The following discussion will show that this observation of a quadruplet around 355 cm^{-1} is entirely consistent with expectations.

The quadruplet is *not* a Davydov multiplet arising from a single intralayer eigenvector. Davydov doublets, not quadruplets, occur in orpiment, and only *one* member of each doublet is Raman-active (the other is infrared-active).² Nor is it a crystal-field multiplet arising from a mode degenerate in the layer symmetry, since the layer symmetry is *too low* to allow degeneracies. In both the layer ($\text{Pnm}2_1$, or DG32 in Wood's compilation⁴ of the diperic groups) and the crystal ($\text{P}2_1/n$) space-group symmetries of As_2S_3 , all modes are nondegenerate. (The infrared-Raman near-degeneracy of Davydov doublets in the crystal is enforced by the validity of the weak-coupling picture.² Symmetry enters only in the sense that the weakness of the layer-layer coupling permits both eigenvectors of a given Davydov doublet to be characterized by the same representation of DG32.) Thus the Raman lines near 355 cm^{-1} arise from *different* intralayer vibrations.

DeFonzo and Tauc, in a detailed analysis, have calculated values of bond-stretching mode frequencies of a single layer.¹¹ They find four modes, one of each of the four layer-symmetry types of DG32 (A_1, A_2, B_1, B_2), near 355 cm^{-1} . In the crystal, these four layer modes must give rise to eight crystal modes. Of these, four will be Raman-active; two of crystal symmetry A_g and two of B_g symmetry.² Now while the initial (isolated-layer limit) modes of a single layer all have different layer symmetries, the resulting four Raman-active crystal modes occur as two pairs of *similar crystal symmetry*. The two A_g modes cannot be degenerate because, being of the same symmetry, they will admix to split any such degeneracy, likewise for the two B_g modes. At $P=0$, this effect is very small because the crystal symmetry is, to good approximation, without influence. However, at high pressure, as each layer is forced to "feel" the presence of its neighboring layers, the crystalline environment starts to

take hold and the admixture effect of like-symmetry modes must split them apart. The above analysis provides the explanation of the results shown in Figs. 4 and 5.

A similar phenomenon occurs in another portion of the spectrum, near 150 cm^{-1} . Here the repulsion effect is most prominent in avoiding like-symmetry degeneracy, not at $P=0$, but at high pressure. At $P=0$, lines are observed at 136 and 154 cm^{-1} . When pressure is applied, the 136-cm^{-1} line begins to shift upward in frequency. Meanwhile the 154-cm^{-1} line splits into two, and its lower-frequency component begins to be overtaken by the line originally at 136 cm^{-1} . The latter two lines appear headed for collision (degeneracy) at about 25 kbar. However, the crossing never happens. The two lines repel each other, the natural explanation being that they correspond to modes of the same crystal symmetry.

The above effects provide definite evidence of the looked-for dimensionality effects discussed in Sec. I. Pressure leaves behind the weak-coupling limit, which is such a good picture at $P=0$ with the layer symmetry dominant, and induces three dimensionality. Put differently, the molecularity of the solid declines at high pressure. Note that the splittings induced by pressure cause certain modes to decrease in frequency.

In connection with the occurrence of negative values of dv/dP for a few intralayer modes, the following observations are relevant. The lines at 289 and 293 cm^{-1} have negative pressure coefficients, as does the lowest-frequency member of the multiplet of Fig. 5 and a weak line at 326 cm^{-1} which was monitored in the earlier low-pressure study.¹⁵ Negative pressure coefficients for internal-mode frequencies have also been observed in pressure-Raman experiments on the chain-structure (1D-network) chalcogen crystals Se and Te.³⁸ Now it is known that in 1D- and 2D-network crystals, it is possible for a molecular dimension to *expand* under hydrostatic compression because the internal strain occurs by a bond-bending deformation (think of an accordionlike motion). This is just what happens in trigonal Se and Te; under pressure, the helical chains actually *increase* in length.

By photographic observation of orpiment crystals while under pressure in the anvil cell, we have obtained rough estimates of the linear compressibilities of As_2S_3 in the layer plane. The results for $-(1/l)(dl/dP)$ are $(2 \pm 0.5) \times 10^{-6}\text{ bar}^{-1}$ and $-(0.1 \pm 0.3) \times 10^{-6}\text{ bar}^{-1}$ in the a and c directions, respectively. The tendency of the layers to expand under pressure in the c direction may be associated, by analogy with Se and Te, with the negative dv/dP seen for some intralayer modes.

V. THE EXPLICIT-IMPLICIT MIX IN THE TEMPERATURE DEPENDENCES

If E denotes a characteristic energy or frequency in a crystal, its observed variation with temperature at constant pressure ($P \approx 0$) can be decomposed into two distinct components:

$$\left(\frac{\partial E}{\partial T}\right)_P = \left(\frac{\partial E}{\partial T}\right)_V - \frac{\alpha}{\beta} \left(\frac{\partial E}{\partial P}\right)_T.$$

Here V is the crystal volume, α is the volume expansivity $(1/V)(\partial V/\partial T)_P$, and β is the compressibility $-(1/V)(\partial V/\partial P)_T$. The left side is the total observed temperature coefficient, usually written simply dE/dT (constant pressure, i.e., $P=0$, being understood). The first term on the right is the "explicit" contribution at constant volume, the "pure" effect of temperature. It reflects the effect of the change in the vibrational amplitudes, i.e., the phonon occupation numbers, at fixed equilibrium positions. The second term, known as the "implicit" contribution, reflects the effect of the change in equilibrium interatomic spacings that accompanies, via thermal expansion, a change in temperature. The implicit term $-(\alpha/\beta)(dE/dP)$ is accessible to experiment through measurement of the pressure coefficient $(dE/dP) = (\partial E/\partial P)_T$.

An analysis of the explicit/implicit dissection of temperature derivatives has been given recently by Zallen and Conwell³⁹ for molecular crystals, for the case of phonon frequencies ($E = \nu$). For highly anisotropic crystals (such as As_2S_3) α and β are not simple scalars, but since these two quantities tend to have similar anisotropies, the anisotropy of their "ratio" is reduced. In any case, since α and β are not known for As_2S_3 , the above relationship is discussed here in a largely qualitative context. For α/β we adopt an approximate value of 1.0×10^{-2} kbar/K, based on the known compressibility⁴⁰ and thermal expansion⁴¹ of the amorphous form of As_2S_3 .

For the electronic bandgap in As_2S_3 , we have found a value of -14 meV/kbar for $(\partial E_G/\partial P)_T = dE_G/dP$. This corresponds to a thermal-expansion-induced implicit contribution $[-(\alpha/\beta)(dE_G/dP)]$ to dE_G/dT which is about $+0.14$ meV/K. In marked contrast to this, the observed total temperature coefficient (near 300 K) is found to be an order of magnitude larger in size and of opposite sign^{6,42}: $dE_G/dT = -1.3$ meV/K. It is therefore evident that it is the *explicit* contribution which dominates dE_G/dT ; in the context of an electronic excitation this is equivalent to the statement that the bandgap temperature coefficient is controlled primarily by the electron-phonon interaction.

For the phonon case, we are in a position to

perform the analogous explicit-implicit decomposition of $d\nu/dT$ for about a dozen Raman-active optical modes. Our results for phonons in As_2S_3 are displayed in Fig. 6 in a graphical representation that has been described elsewhere by Zallen and Conwell.³⁹ In this type of plot, each individual point represents a phonon mode; the point is positioned according to the pressure (x axis) and temperature (y axis) derivatives of the mode frequency near $P=0$, $T=300$ K. For mode i , $x_i = (\partial \nu_i/\partial P)_T = (d\nu_i/dP)$, and $y_i = -(\partial \nu_i/\partial T)_P = -(d\nu_i/dT)$. In such a diagram, straight lines through the origin define loci along which the explicit-implicit mix in $d\nu/dT$ is constant. We have labeled several such "isomix" lines by the value of the dimensionless parameter η , the *implicit fraction* specifying the ratio of the volume-driven term to the total temperature dependence:

$$\begin{aligned} \eta &= -\frac{\alpha(d\nu)}{\beta(dP)} \left(\frac{d\nu}{dT}\right)^{-1} \\ &= 1 - \left(\frac{\partial \nu}{\partial T}\right)_V \left(\frac{d\nu}{dT}\right)^{-1}. \end{aligned}$$

In terms of the above "coordinates" (x_i, y_i), a mode i with implicit fraction η_i satisfies $y_i = \eta_i^{-1}(\alpha/\beta)x_i$. Thus phonons corresponding to the volume-driven implicit-dominated situation with $\eta_i = 1$ lie along a line of slope α/β in Fig. 6, while phonons corresponding to the explicit-dominated $\eta_i = 0$ situation lie along a vertical line.

In order to provide a standard of comparison for our results on As_2S_3 , the upper half of Fig. 6 reproduces data for crystalline As_4S_4 ,^{36,39} a chemically similar but structurally different As-S solid composed of eight-atom nearly spherical cagelike molecular units. In addition to its compositional kinship to orpiment, As_4S_4 is relevant because its explicit-implicit behavior is well documented and is typical of molecular crystals. The solid dots denote external-mode phonons, all with frequencies below 65 cm^{-1} , while the open triangles denote internal-mode phonons with frequencies above 300 cm^{-1} . For the external modes, there is seen to be a high correlation between the sensitivity to pressure and the sensitivity to temperature, and the trend line is not far from the $\eta = 1$ case corresponding to thermal-expansion-dominated behavior in which $d\nu/dT$ is close to the implicit contribution $-(\alpha/\beta)(d\nu/dP)$. For the high-frequency intramolecular modes, the explicit contribution is more important as η is closer to 0 than 1.

Our analogous data for orpiment is shown in the lower part of Fig. 6. Included here are the modes with ν less than 70 cm^{-1} as well as those with ν above 280 cm^{-1} . The low-frequency modes, in

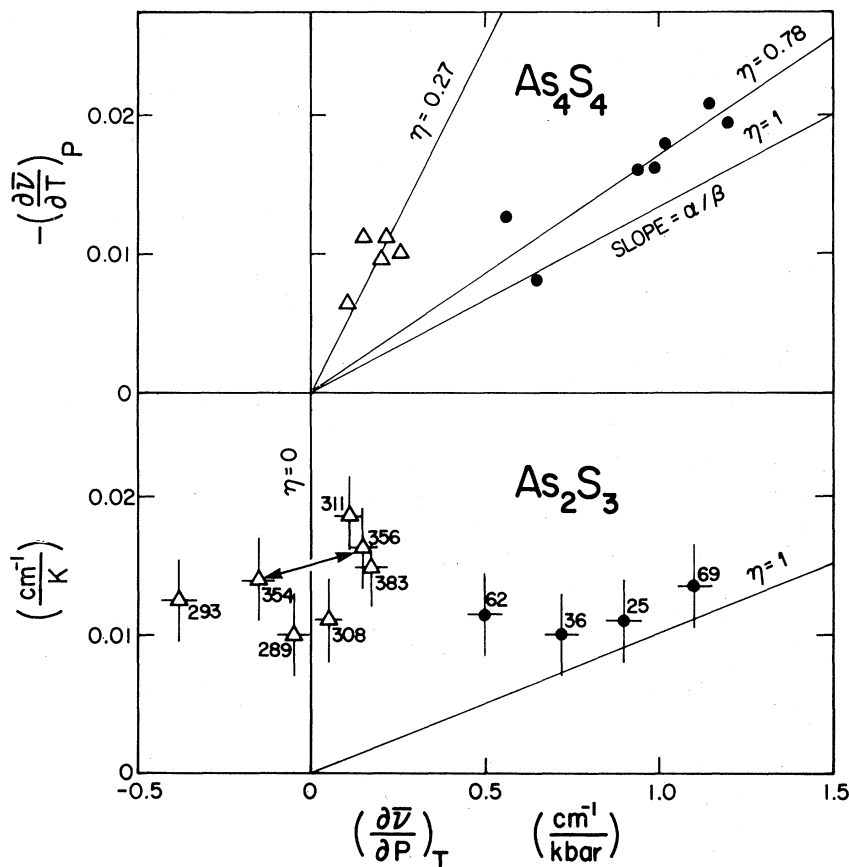


FIG. 6. The correlation between the temperature and pressure derivatives of phonon frequencies for As_2S_3 , compared to the corresponding correlation in As_4S_4 (Ref. 39). Each point represents a Raman-active optical mode whose frequency has been followed as a function of temperature (at $P \approx 0$) and of pressure (at $T \approx 300$ K). The solid dots denote interlayer (intermolecular) modes at low frequencies (<70 cm^{-1}) for As_2S_3 (As_4S_4), while the open triangles denote intralayer (intramolecular) modes at high frequencies (>280 cm^{-1}). Straight lines define loci of constant explicit-implicit mix in dv/dT , and are labeled by the implicit fraction η .

which the interlayer interactions play the dominant role, are the layer-crystal analogs of intermolecular (external) modes. The high-frequency modes, clustered in the vicinity of $300\text{--}360$ cm^{-1} , correspond to covalent bond stretching. Intermediate-frequency ($70 < \nu < 280$ cm^{-1}) modes have been omitted from Fig. 6 for clarity; the behavior of these bond-bending modes is generally intermediate between that exhibited by the interlayer and the bond-stretching intralayer modes. The pressure coefficients for the modes at 289, 308, 354, and 356 cm^{-1} are from the present study; the others are from the accurate low-pressure data of Ref. 15. Temperature coefficients are from Ref. 13 and from previously unreported results which were obtained in the course of that earlier study. As indicated by the error bars, the temperature coefficients are less accurately known than the pressure ones.

For the interlayer modes, the overall behavior is seen to be similar to that found in the simpler

(nearly isotropic, small-molecule) case of As_4S_4 . Although this analysis is approximate because the high crystal anisotropy complicates the interpretation of the expansivity-compressibility ratio α/β , the low-frequency modes are clearly characterized by η values which are closer to 1 than to 0. The thermal-expansion-induced, volume-driven, implicit effect dominates for the interlayer modes, as has been documented to be the case for intermolecular (external) modes by Zallen and Conwell.³⁹

For the high-frequency intralayer modes of orpiment, the situation is much less well-defined than for the intramolecular modes in As_4S_4 . For the latter, all modes have dv/dP positive and dv/dT negative, so that the explicit and implicit contributions have the same sign. Quantitatively, the magnitude of the explicit term is larger than that of the implicit term. For As_2S_3 , dv/dP is negative for some modes, a circumstance which we have associated with the severe anisotropy in

a layer crystal (e.g., one intralayer dimension actually expands under pressure). There is little correlation between dv/dT and dv/dP . Nevertheless, the region occupied by the cluster of open triangles in the As_2S_3 map in Fig. 6 is contained within a sector which brackets $\eta = 0$ (roughly given by $-0.3 < \eta < +0.2$) and which does *not* overlap the sector (roughly given by $+0.6 < \eta < +0.9$) containing the pressure-sensitive low-frequency modes. Thus the intralayer bond-stretching modes and the interlayer modes are distinguished from each other with respect to their explicit-implicit mix, just as they are mutually distinct in several other respects. Although the spread in η is much larger for the intralayer modes in As_2S_3 than for the analogous intramolecular modes in As_4S_4 , it remains true that η is closer to 0 than 1 so that the explicit effect dominates. Note that a small and *negative* η means that the implicit term is not only small in size but is also opposite in sign to the total dv/dT , having been overridden by the larger explicit term (in a situation similar to that found earlier for the bandgap).

In Fig. 6, the two triangles linked by arrowheads correspond to the lowest two components of the 355 cm^{-1} quadruplet. The pressure-induced dispersion of the multiplet (shown previously in Fig. 5) has the effect of spreading the points out along the dv/dP axis in Fig. 6, pushing the lowest into negative territory.

VI. SUMMARY

Using the diamond-anvil-cell technique, we have measured the effect of pressure, at room temperature, on the optical absorption edge and the Raman scattering spectrum of orpiment. With increasing pressure the optical band gap red-shifts rapidly, decreasing from 2.7 eV at $P = 0$ to 1.6 eV at 100 kbar. The initial slope, dE_G/dP at $P = 0$, is $-(14 \pm 3)$ meV/kbar. The closing of the gap is interpreted in terms of pressure-induced enhancement of the interlayer-interaction broadening of intralayer bands, which is a common char-

acteristic of semiconducting layer crystals.

The effect on Raman frequencies is greatest for the rigid-layer modes, which approximately double in frequency by 100 kbar, corresponding to a quadrupling of the interlayer force constants. Enhanced three-dimensionality is also manifest in the high-frequency part of the vibrational spectrum. A multiplet at 355 cm^{-1} , near degenerate (to within 5 cm^{-1}) at $P = 0$ because of the weakness of the layer-layer coupling, splits substantially ($> 30\text{ cm}^{-1}$) at high pressure as the dominance of the diperic layer symmetry is broken and the admixture repulsion of like-symmetry crystal modes forces them apart. A similar effect occurs at 25 kbar in a forbidden-crossover repulsion of a pair of modes at 145 cm^{-1} .

Finally, the pressure data have been used to separate the phonon-occupation-driven (explicit) and the volume-driven (implicit) contributions to the temperature dependence of the band gap and the Raman-active phonon frequencies. E_G is controlled by the explicit contribution to dE_G/dT , which in an electronic context corresponds to the dominance of the electron-phonon interaction. For the phonons, dv/dT of the low-frequency interlayer-interaction modes is dominated by the volume-driven term, while the phonon-phonon explicit effect plays the major role in the more varied behavior exhibited by the intralayer modes.

ACKNOWLEDGMENTS

The authors are indebted to A. Rimsky (Laboratoire de Mineralogie et Cristallographie, Université Pierre-et-Marie Curie, Paris) for providing and for characterizing some of the orpiment samples used in this work. We also wish to thank F. Mollot (GPS-ENS) for his help with the absorption measurements and for useful discussions about the results. One of us (R.Z.) wishes to express his appreciation to the Laboratoire de Physique des Solides for that group's splendid hospitality.

*Laboratoire associé au CNRS.

¹N. Morimoto, *Mineral. J.* **1**, 160 (1954); A. A. Vaipolin, *Kristallografiya* **10**, 596 (1965) [*Sov. Phys.—Crystallogr.* **10**, 509 (1966)]; D. J. E. Mullen and W. Nowacki, *Z. Kristallogr.* **136**, 48 (1972).

²R. Zallen, M. L. Slade, and A. T. Ward, *Phys. Rev. B* **3**, 4257 (1971); R. Zallen, in *Proceedings of the Twelfth International Conference on the Physics of Semiconductors, Stuttgart, 1974*, edited by M. H. Pilkuhn (Teubner, Stuttgart, 1974), p. 621.

³The 80 diperic space groups are the appropriate groups for describing three-dimensional objects which

are translationally periodic in two dimensions and non-periodic (e.g., finite in extent) in the third. Such symmetry applies, quite rigorously, to an individual covalently-bonded macromolecular layer in a layer-structure crystal. In effect, the applicable diperic factor group constitutes the "molecular symmetry" for a layer crystal; it is a factor-group symmetry instead of a point-group symmetry because here the "molecule" is macroscopically extended in two dimensions. An enumeration and description of the 80 diperic groups has been given by Wood (Ref. 4).

⁴E. A. Wood, *Bell Syst. Tech. J.* **43**, 541 (1964); Bell

- Teleph. Syst. Tech. Publ. Monographs 4680, 1964 (unpublished). The monograph, which contains the complete description of the 80 diaperiodic groups, is available as NAPS document No. 02655 from the National Auxiliary Publications Service of the American Society for Information Science (ASIS/NAPS, P.O. Box 3513, Grand Central Station, New York, N. Y. 10017).
- ⁵W. H. Zachariasen, *J. Am. Chem. Soc.* **54**, 3841 (1932). Figure 1 of this paper is the famous diagram in which Zachariasen used a hypothetical A_2B_3 compound to provide a two-dimensional analogy for his ideas on the structural relation between the crystalline and glassy forms of a given material. As_2S_3 is a physical realization of the bonding topology sketched in that figure.
- ⁶R. Zallen, R. E. Drews, R. L. Emerald, and M. L. Slade, *Phys. Rev. Lett.* **26**, 1564 (1971); *Solid State Commun.* **10**, 293 (1972).
- ⁷G. Lucovsky, *Phys. Rev. B* **6**, 1480 (1972).
- ⁸P. C. Taylor, S. G. Bishop, D. L. Mitchell, and D. Treacy, in *Proceedings of the Fifth International Conference on Amorphous and Liquid Semiconductors*, edited by J. Stuke and W. Brenig (Taylor and Francis, London, 1974), p. 1267.
- ⁹P. B. Klein, P. C. Taylor, and D. J. Treacy, *Phys. Rev. B* **16**, 4501 (1977); **16**, 4511 (1977).
- ¹⁰D. Treacy and P. C. Taylor, *Phys. Rev. B* **11**, 2941 (1975).
- ¹¹R. Forneris, *Am. Mineral.* **54**, 1062 (1969); J. P. Mathieu and H. Poulet, *Bull. Soc. Fr. Mineral Crystallogr.* **93**, 532 (1970); A. P. DeFonzo and J. Tauc, *Phys. Rev. B* **18**, 6957 (1978); C. Razetti and P. P. Lottici, *Solid State Commun.* **29**, 361 (1979).
- ¹²R. J. Kobliska and S. A. Solin, *Phys. Rev. B* **8**, 756 (1973).
- ¹³R. Zallen and M. L. Slade, *Phys. Rev. B* **9**, 1627 (1974).
- ¹⁴O. L. Kukhto, V. I. Mikhailov, R. P. Ozerov, and S. P. Solov'ev, *Fiz. Tverd. Tela (Leningrad)* **18**, 1707 (1976). [*Sov. Phys.—Solid State* **18**, 991 (1976)].
- ¹⁵R. Zallen, *Phys. Rev. B* **9**, 4485 (1974).
- ¹⁶B. L. Evans and P. A. Young, *Proc. R. Soc. London, Ser. A* **297**, 230 (1967).
- ¹⁷D. F. Blossey and R. Zallen, *Phys. Rev. B* **9**, 4306 (1974).
- ¹⁸R. Zallen and D. F. Blossey, in *Optical and Electrical Properties of Compounds with Layered Structures*, edited by P. A. Lee (Reidel, Dordrecht, 1976), p. 231.
- ¹⁹S. G. Bishop and N. J. Shevchik, *Phys. Rev. B* **12**, 1567 (1975); W. R. Salaneck and R. Zallen, *Solid State Commun.* **20**, 793 (1976).
- ²⁰J. Perrin, J. Cazaux, and P. Soukiassian, *Phys. Status Solidi B* **62**, 343 (1974).
- ²¹L. B. Schein, *Phys. Rev. B* **15**, 1024 (1977).
- ²²G. J. Piermarini and S. Block, *Rev. Sci. Instrum.* **46**, 973 (1975); G. J. Piermarini, S. Block, J. D. Barnett, and R. A. Forman, *J. Appl. Phys.* **46**, 2774 (1975).
- ²³J. M. Besson and J. P. Pinceaux, *Rev. Sci. Instrum.* **50**, 541 (1979).
- ²⁴W. Paul, in *The Optical Properties of Solids, Proceedings of the International School of Physics, "Enrico Fermi," Course XXXIV*, edited by J. Tauc (Academic, New York, 1966), p. 257; R. Zallen and W. Paul, *Phys. Rev.* **155**, 703 (1967); W. Paul in *Propriétés Physiques des Solides sous Pression* (CNRS, Paris, 1970), p. 199; G. Martinez, in *Handbook of Semiconductors* (North-Holland, Amsterdam, 1980), Vol. 2.
- ²⁵J. M. Besson, K. P. Jain, and A. Kuhn, *Phys. Rev. Lett.* **32**, 936 (1974).
- ²⁶J. M. Besson, *Nuovo Cimento* **38B**, 478 (1977); M. J. Powell and A. J. Grant, *ibid.* **38B**, p. 486 (1977); C. Carillon and G. Martinex, *ibid.* **38B**, p. 496 (1977).
- ²⁷A. J. Grant and A. D. Yoffe, *Solid State Commun.* **8**, 1919 (1970); B. T. Kolomiets and E. M. Raspopova, *Fiz. Tekh. Poluprovodn.* **4**, 157 (1970) [*Sov. Phys.—Semicond.* **4**, 124 (1970)].
- ²⁸M. P. Lisitsa, A. M. Yaremko, G. G. Tarasov, M. Ya. Valakh, and L. I. Berezhinski, *Fiz. Tverd. Tela (Leningrad)* **14**, 2744 (1973) [*Sov. Phys.—Solid State* **14**, 2744 (1973)].
- ²⁹Network dimensionality is here defined as the number of dimensions in which the covalently-bonded molecular unit is *macroscopically extended*. A further discussion of this concept can be found in the second entry of Ref. 2.
- ³⁰A. I. Gubanov and S. M. Dunaevski, *Fiz. Tekh. Poluprovodn.* **8**, 716 (1974) [*Sov. Phys.—Semicond.* **8**, 457 (1974)].
- ³¹H. L. Althaus, G. Weiser, and S. Nagel, *Phys. Status Solidi B* **87**, 117 (1978); G. Weiser in *Physics of Selenium and Tellurium*, edited by E. Gerlach and P. Grosse (Springer, Berlin, 1979), p. 230.
- ³²E. Mooser and W. B. Pearson, in *Progress in Semiconductors*, edited by A. F. Gibson, R. E. Burgess, and F. A. Kroger (Wiley, New York, 1960), Vol. V, p. 104.
- ³³M. Kastner, *Phys. Rev. Lett.* **28**, 355 (1972); *Phys. Rev. B* **7**, 5237 (1973).
- ³⁴In the 3D-network semiconductors of the germanium family, it is true that the (antibonding) conduction band broadens more than the (bonding) valence band under pressure (see Ref. 24). If Althaus *et al.* (Ref. 31) are correct about the bonding character of the uppermost valence band in As_2Se_3 , then that pressure-sensitivity situation could apply to this chalcogenide.
- ³⁵B. A. Weinstein, R. Zallen, and M. L. Slade, *J. Non-Cryst. Solids* **35 & 36**, 1255 (1980); K. Aoki, O. Shimomura, and S. Minomura, in *Proceedings of the Fourth International Conference on High Pressure* (Physico-Chemical Society of Japan, Kyoto, 1975), p. 314.
- ³⁶R. Zallen and M. L. Slade, *Phys. Rev. B* **18**, 5775 (1978).
- ³⁷The "record," thus far, for the pressure-induced blue-shifting of RL modes is held by GaS. At 170 kbar the RL mode has more than tripled in frequency, corresponding to an order of magnitude increase in restoring force. A. Polian, K. Kunc, and A. Kuhn, in *Proceedings of the XIII International Conference on the Physics of Semiconductors, Rome, 1976*, edited by F. G. Fumi (Tipografia Marves, Rome, 1976), p. 392.
- ³⁸W. Richter, J. B. Renucci, and M. Cardona, *Phys. Status Solidi B* **56**, 223 (1973).
- ³⁹R. Zallen and E. M. Conwell, *Solid State Commun.* **31**, 557 (1979).
- ⁴⁰D. Gerlich, E. Litov, and O. L. Anderson, *Phys. Rev. B* **20**, 2529 (1979).
- ⁴¹T. N. Claytor and R. J. Sladek, in *Proceedings of the Sixth International Conference on Amorphous and Liquid Semiconductors, Leningrad, 1975*, (Acad. Sci. USSR, Leningrad, 1976), p. 54.
- ⁴²J. R. Zakis and H. Fritzsche, *Phys. Status Solidi B* **64**, 123 (1974).